The nonlocality of coupling and the retrieval of field-correlations with arrays of waveguides

Stefano Minardi
Institute of Applied Physics, Friedrich-Schiller Universität, Max-Wien Platz 1, D-07745 Jena, Germany.

Arrays of evanescently coupled waveguides can be used to retrieve simultaneously the first order correlation functions in multiple-field interferometry. Here it is shown that this remarkable property of waveguide arrays is enabled only by the existence of non-local interaction, *i.e.* non-nearest-neighbor coupling between the waveguides.

PACS numbers: 42.82.Et, 42.25.Hz, 42.25.Kb

I. INTRODUCTION

Classical interferometry usually deals with the analysis of the interference of a single pair of wave fields. However, there are important applications in which the simultaneous interference of multiple wave fields is of relevance, like stellar interferometry [1], the verification of the foundations of quantum mechanics [2], or multichannel phase measurements in biosensors [3]. In all these cases, the retrieval of the mutual field-correlation functions (also known as complex visibility) from the measurement of an interference pattern is required. The interference pattern can be generated by a multi-beam Young interferometer [2, 3], or by a suitably designed, planar integrated optical circuit [4]. Recently, it was shown that two-dimensional (2D) arrays of evanescently coupled, single-mode waveguides can be used for the same purpose [5–7].

One dimensional (1D) and 2D arrays of evanescently coupled waveguides are the optical analogues of 1D and 2D tight-binding, solid-state quantum systems [8], respectively. They were used to explore fundamental aspects of solid-state physics [9], quantum [10] and nonlinear classical optics [11, 12], but also in applications such as saturable absorbers for mode-locked lasers [11, 13]. From the theoretical viewpoint, arrays of coupled waveguides are usually treated in terms of nearest-neighbor coupling. However, non-nearest-neighbor (NNN) interaction becomes relevant for 2D square arrays, through the coupling along the diagonal direction. In solid state systems, NNN coupling is characteristic of long-range, spatially nonlocal potentials. In optics, NNN interaction was investigated in zig-zag arrays of waveguides and found to influence the transport of light within the array for single waveguide excitation [14]. NNN was also proved to be an essential feature of arrays of waveguides used to simulate optically an extended Hubbard model [15]. In nonlinear systems, NNN coupling enables the existence of higher order discrete solitons with nontrivial phase profile, including *e.g.* discrete vortex solitons of topological charge larger than unity [16].

In this article, I show that NNN coupling has a dramatic impact on the capability of a finite waveguide array to retrieve the first-order correlation functions of multiple input fields. Indeed, an array of waveguides with only nearest neighbor coupling cannot be used to retrieve the complex visibilities of the input beams. On the contrary, the inclusion of NNN coupling allows the array to act as a well-conditioned multichannel coherence sensor for some input field configuration and array length. I show further that this behavior is related to the fact that, in the case of NNN coupling, the phase of the discrete input-response function of the array is not bounded to a discrete set (like in the nearest-neighbor interaction case), but can take virtually any value. In particular, the presence of NNN coupling breaks the spatial symmetry of the phase pattern in the input-response function, which is typical of nearest-neighbor coupled arrays. The symmetry breaking eventually allows the simultaneous retrieval of all the mutual correlation functions of the multiple excitation fields.

The paper is structured as follows: in Section II, I recall the mathematical formalism necessary to handle the problem of multi-field interferometry with arrays of waveguides. In section III, I describe the impact of NNN coupling on the capability of the array to retrieve the coherence information of the exciting fields. Section IV is devoted to a recall of the analytical solutions of the light propagation in general arrays of coupled waveguides. In section V, I prove through numerical simulations that the symmetry breaking of the phase pattern of the input-response function of the array is a necessary condition for the array to act as a coherence sensor for multi-field interferometry. Finally, conclusions are drawn and further applications of the results are outlined.

II. ARRAYS OF WAVEGUIDES AS MULTIFIELD INTERFEROMETERS

Figure 1(a), illustrates how to retrieve the coherence properties of multiple input fields (in this case, 4) by means of an array of coupled waveguides. Each of the input fields is coupled to a different waveguide at the input facet of the array. The light propagates then in the array and the multi-field discrete interference pattern is detected by an array of detectors, each matching the output of a single waveguide. By choosing appropriately the input waveguides and the propagation length in the array, it's possible to relate uniquely the detected output power pattern to all possible first-order mutual

correlation functions of the input fields (complex visibilities). The device is usually addressed as the discrete beam combiner (DBC), a name which stresses the role of light propagation in discrete optics (the arrays of coupled waveguides, [17]) as underlying principle of the retrieval of the coherence properties of light.

I recall now the mathematical formalism which describes quantitatively the operation of the waveguide array as multi-field interferometer [5]. Light propagation in an array of N identical, single-mode waveguides is usually treated in the frame of the coupled modes approximation. In this approximation, it is considered that the neighboring waveguides perturb only the complex amplitude $a_{\rm n}$ of the mode propagating in a given waveguide n. As a result, the mode amplitudes evolve along the propagation coordinate z according to a set of N coupled equations:

$$i\partial_z a_{\rm n} = \beta a_{\rm n} + \sum_{\rm k\neq n} C_{\rm nk} a_{\rm k}, \tag{1}$$

were $C_{\rm nk}$ is a matrix describing the coupling between the modes n and k. β is the propagation constant of the mode, which is the same for all waveguides. As illustrated in Fig. 1(b), for a given waveguide, only three types of coupling are relevant in a 2D array. We have the nearest-neighbor interaction, which are characterized by the horizontal and vertical coupling coefficients (C_h and C_v), and the non-nearest neighbor interaction, characterized by the diagonal coupling coefficient C_d. In a linear 1D array, we can usually neglect NNN interaction and the same formalism of Eq. (1) holds provided only the horizontal coupling is retained ($C_v = C_d = 0$).

The general solution of the system of equation (1) can be cast in the following form:

$$a_{\rm n}(z) = e^{-i\beta z} \sum_{\rm k=1}^{N} U_{\rm nk}(z) a_{\rm k}(0), \tag{2}$$

where the complex matrix $U_{\rm nk}(z)$ is referred to as the input-response function of the array. Indeed, $U_{\rm nk}(z)$ is the amplitude of the mode n at the propagation distance z, resulting from the excitation of waveguide k. The input-response function of the array can be obtained from direct integration of Eq. (1) or calculated analytically (see Section IV). We notice that if $a_{\rm k}(0)$ is finite for several k (*i.e.* we are simultaneously exciting many waveguides), the output fields $a_{\rm n}(z)$ result from a multiple-field interference. Moreover, it is easy to demonstrate that the power carried by the mode $a_{\rm n}(z)$ is a linear combination of all possible field-correlation functions of the input fields $\Gamma_{\rm ij} = \langle a_{f({\rm i})}(0) a^*_{f({\rm j})}(0)\rangle$ [5], with i, j $= 1...M$, M being the number of simultaneously excited waveguides and f is a function mapping $\{1...M\}$ into the N indices of the waveguides. By convention, we count the waveguide sites as seen from the output facet of the array from left to right and top to bottom (see also numbering in Fig. 1(a)).

Provided we transform the field-correlation functions in their quadratures, we can write the output mode-

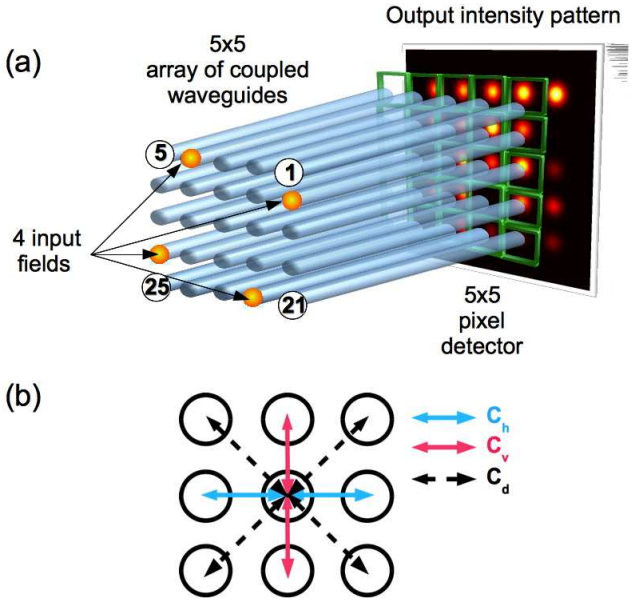

FIG. 1. (Color online) (a) Cartoon illustrating the setup allowing the simultaneous retrieval of the field-correlation functions of 4 light fields injected in selected waveguides of a square array of 5 × 5 coupled waveguides. The chosen numbering of the waveguides is overlaid. (b) Definition of the relevant coupling coefficients in a square array of waveguides.

power pattern in terms of a real-valued vector-matrix multiplication:

$$P_{\rm n}(z) = |a_n(z)|^2 = \sum_{\rm k=1}^{M^2} \alpha_{\rm n,k}(z) G_{\rm k}, \tag{3}$$

where the M^2 -element vector containing the quadratures of the field-correlation functions is defined as [5]:

$$G_{\rm k} = \Gamma_{\rm kk} \quad k = 1...M \tag{4a}$$

$$G_{\rm j+(k-1)\cdot(k-2)/2+M} = Re\{\Gamma_{\rm jk}\} \quad {\rm j} < {\rm k} \quad k = 2...M \tag{4b}$$

$$G_{\rm j+(k-1)\cdot(k-2)/2+M(M+1)/2} = Im\{\Gamma_{\rm jk}\} \quad {\rm j} < {\rm k} \quad k = 2...M \tag{4c}$$

The elements of the matrix $\alpha_{\mathrm{n,k}}$ are related to the elements $\{U\}$ by:

$$\alpha_{\mathrm{n,k}} = |U_{\mathrm{n},f(\mathrm{k})}|^2 \quad k = 1...M \tag{5a}$$

$$\alpha_{\mathrm{n,j+(k-1)\cdot(k-2)/2+M}} = 2Re\{U_{\mathrm{n},f(\mathrm{j})}U^*_{\mathrm{n},f(\mathrm{k})}\} \quad \mathrm{j} < \mathrm{k} \quad \mathrm{k} = 2...M \tag{5b}$$

$$\alpha_{\mathrm{n,j+(k-1)\cdot(k-2)/2+M(M+1)/2}} = -2Im\{U_{\mathrm{n},f(\mathrm{j})}U^*_{\mathrm{n},f(\mathrm{k})}\} \quad \mathrm{j} < \mathrm{k} \quad \mathrm{k} = 2...M \tag{5c}$$

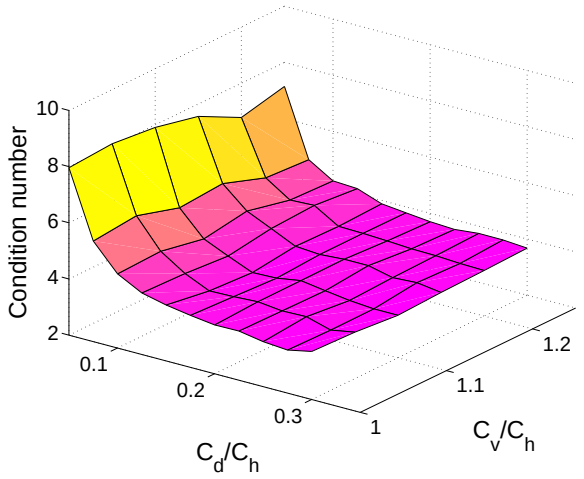

FIG. 2. (Color online) Best condition number of the α-matrix as a function of the relative diagonal and vertical coupling strength.

For $N \geq M^2$, Eq. (3) represents an (over)-determined system of equation which relates the output power pattern $P_{\mathrm{n}}(z)$ to the first-order coherence state G_{k} of the input fields. If the matrix $\{\alpha\}$ is well conditioned for a certain propagation distance z and input configuration f, we can find its (pseudo)-inverse and retrieve the coherence state of the input fields from measurements of their discrete interference pattern $P_{\mathrm{n}}(z)$.

As a gauge of the conditioning, we will use the condition number (CN) of the matrix, defined as the ratio between the maximal and the minimal singular value of the matrix [18]. The smaller the CN, the better conditioned is the matrix. For practical purposes, we define the α-matrix as well conditioned if the CN is below ~ 10.

III. EFFECT OF NNN COUPLING ON THE RETRIEVAL OF THE FIELD CORRELATION FUNCTIONS

To illustrate the effect of the NNN coupling on the retrieval of the field correlation functions, I performed several numerical simulations for a specific realization of the array of waveguides. In particular, I analyzed the properties of a $M = 4$ field combination in a 2D array of waveguides featuring $N = 5 \times 5 = 25$ waveguides. Although an array of 4×4 waveguides is sufficient to retrieve the coherence of $M = 4$ optical fields [5], it was shown that 2D arrays featuring $N = (M+1) \times (M+1)$ waveguides has a significantly smaller condition number than arrays featuring only $N = M^2$ [19].

In the fist simulation, I keep the horizontal coupling constant and investigate the impact of the vertical and diagonal coupling on the conditioning of the α-matrix. Figure 2 illustrates a scan of the best condition number for the α-matrix of the investigated system as a function of the diagonal and vertical coupling coefficients. The best values were calculated within a maximum propagation length $z_{\max} = \pi/C_h = 2L_h$ (L_h is the horizontal coupling length of the array). From the graph, two conclusions can be drawn, namely *i)* the strength of the diagonal coupling influences the condition number more than the vertical coupling strength, and *ii)* for vanishing diagonal coupling, the condition number increases steeply. In fact, by setting the diagonal coupling exactly to 0, the condition number becomes infinite and the pseudo-inverse of the α-matrix does not exist. The same situation happens by simulating the case of a linear array of waveguides with only nearest neighbor coupling.

To gain insight in the mechanism responsible for these observations, I analyze the α-matrix extracting two quantities from its coefficients. I consider first the cross-correlation terms of the input-response function $\{U_{\mathrm{n},f(\mathrm{j})}U^*_{\mathrm{n},f(\mathrm{k})}\}$ ($\mathrm{j} \neq \mathrm{k}$), whose real and imaginary parts are the elements of the α-matrix (see Eq. 5 (b) and (c)). These elements identify the weights of the quadratures of the field correlation function Γ_{jk} in the sum representing the output power carried by the n^{th} waveguide of the array. For each cross-correlation term it is possible to define an interferometric phase $\Phi_{\mathrm{njk}} = \arg\{U_{\mathrm{n},f(\mathrm{j})}\} - \arg\{U_{\mathrm{n},f(\mathrm{k})}\}$, which is actually the phase delay between the interfering fields observed at site n and injected in sites $f(\mathrm{j})$ and $f(\mathrm{k})$. Next, we define the auto-correlation terms of the input-response function $A_{\mathrm{nj}} = |U_{\mathrm{n},f(\mathrm{j})}|^2$ (first M columns of the α-matrix). The auto-correlation terms describe the weight of the intensity of the field j in the waveguide n. Trivially, the amplitude of the cross-correlation terms of the input response function $\{U_{\mathrm{n},f(\mathrm{j})}U^*_{\mathrm{n},f(\mathrm{k})}\}$ is given by $\sqrt{A_{\mathrm{nj}}A_{\mathrm{nk}}}$.

For a given α-matrix, I consider now the $N \times M \times (M-1)/2$ phases Φ_{njk} and the $N \times M$ intensities A_{nj} as a statistical ensamble and evaluate their histograms for decreasing diagonal coupling (see Fig. 3), along with a comparison of the condition number of the α-matrix. As for the test, I have chosen again the α-matrix corresponding to a $N = 5 \times 5$, 2D array of waveguides with $M = 4$ exciting fields at waveguides 4, 6, 20 and 22 The length of the array has also been fixed to $z_{\max} = 0.88 \cdot L_h$

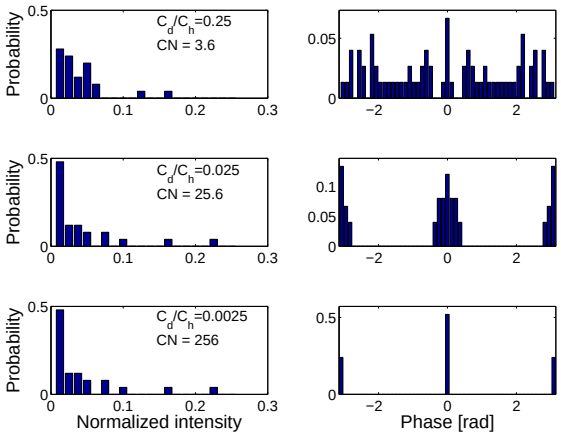

FIG. 3. Histograms of the intensity and phase of the α-matrix elements (see text for details) for three different values of the diagonal coupling for a 5×5 array excited in 4 different points (waveguides 4, 6, 20, 22). The propagation length has been fixed to $z_{\max} = 0.88 \cdot L_h$.As described in the labels, the condition number (CN) of the α-matrix decreases with increasing diagonal coupling.

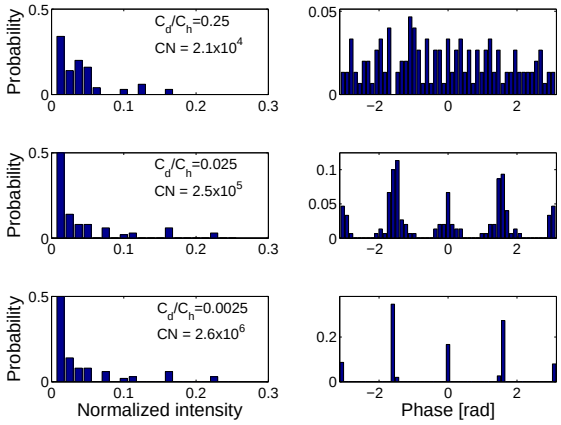

FIG. 4. Histograms of the intensity and phase of the α-matrix elements (see text for details) for three different values of the diagonal coupling for a 5×5 array excited in 4 different points (waveguides: 1, 2, 3, 4). The propagation length has been fixed to $z_{\max} = 0.88 \cdot L_h$. Also in this case, the condition number of the α-matrix is lower for larger diagonal coupling.

and $C_h = C_v$ (vertical and horizontal coupling are equal). With $C_d/C_h = 0.25$, the chosen configuration gives the best conditioned α-matrix with CN=3.6. From Fig. 3 we notice that the phases of the matrix are nearly evenly distributed within the interval $[-\pi, +\pi)$, while the intensities are mainly concentrated at low levels. By repeating the statistics with a ten times smaller diagonal coefficient ($C_d/C_h = 0.025$) we notice that the condition number has increased to CN=25.6 and the phases are more concentrated around the values of $\{0, \pi\}$, while the intensities are not affected significantly. For even weaker diagonal coefficient ($C_d/C_h = 0.0025$), the condition number has grown to CN=256, and all phases are narrowly distributed around positions $\{0, \pi\}$.

For an arbitrary chosen input configuration $f(\mathrm{j})$, the CN is extremely high, nonetheless the nearly uniform distribution of phases as compared to the discrete set reduces the CN (see Fig.4) dramatically.

From these numerical experiments we may conclude that the effect of the NNN coupling is to transform the distribution of the phases Φ_{njk} from a discrete set to a continuous interval of values. This transition is also correlated with a decrease of the condition number with increasing NNN coupling. To explain these observations, we need however to have a look at the analytical description of the input-response function.

IV. PHASE OF THE INPUT-RESPONSE FUNCTION OF THE ARRAY OF WAVEGUIDES

In this Section, I discuss the phase properties of the input-response function for a general array of coupled waveguides. For the $N = (\mu+1) \times (\nu+1)$ array of waveguides with diagonal coupling coefficient C_d the input-response function is [20]:

$$U_{g(\mathrm{m,n}),g(\mathrm{m}',\mathrm{n}')} = i^{\mathrm{m+n+m}'+\mathrm{n}'} \sum_{\mathrm{k,l},\alpha,\gamma=0}^{\infty} i^{\mathrm{k+l}}(-1)^{\alpha\mu+\gamma\nu+k} \times D_{\mathrm{k,l}}(C_d, z) \cdot H_{\mathrm{m,m}',\mathrm{k,l},\alpha,\mu}(C_h, z) \cdot V_{\mathrm{n,n}',\mathrm{k,l},\gamma,\nu}(C_v, z), \quad (6)$$

where C_h and C_v are the horizontal and vertical coupling coefficient. The function $g(\mathrm{m,n})$ maps the waveguide site coordinates $(\mathrm{m,n})$ into a progressive number from 1 to N. Finally, the functions D, H and V take real values and are defined as follows:

$$D_{\mathrm{k,l}}(C_d, z) = J_k(2C_d z) J_l(2C_d z) \tag{7}$$

$$H_{\mathrm{m,m',k,l},\alpha,\mu}(C_h, z) = \left[(-1)^{-m'-k-l} J_{m-m'-k-l+2\alpha(\mu+2)}(2C_h z) + J_{m-m'+k+l+2+2\alpha(\mu+2)}(2C_h z)\right] \tag{8}$$

$$V_{\mathrm{n,n',k,l},\gamma,\nu}(C_v, z) = \left[(-1)^{-n'-k-l} J_{n-n'-k+l+2\gamma(\nu+2)}(2C_v z) + J_{n-n'+k-l+2+2\gamma(\nu+2)}(2C_v z)\right]. \tag{9}$$

Here, $J_k(z)$ indicates the Bessel function of the first kind and index k. We now discuss Eq. (6) for two different cases. First, we consider the linear 1D array with nearest neighbor interaction by setting $C_d = C_v = 0$, second, we analyze the case of the 2D array with no diagonal coupling ($C_d = 0$).

For $C_d = 0$, the only non-vanishing term in the summation on indices k and l in Eq. (6) is the case $\mathrm{k} = \mathrm{l} = 0$. Thus, for the linear array of $\mu + 1$ waveguides the field amplitude at the waveguide m excited at site m' reduces to:

$$U_{\mathrm{m,m'}}(z) = i^{\mathrm{m+m'}} \sum_{\alpha=0}^{\infty} (-1)^{\alpha\mu} H_{\mathrm{m,m',0,0},\alpha,\mu}(C_h, z). \tag{10}$$

It is evident that the input-response function is a complex number given by the product of a real number and the imaginary unit elevated to an integer exponent. Therefore the phase can only take a value from the discrete set $S = \{0, \pi/2, \pi, 3\pi/2\}$. Along propagation, we can have a flip by π of the phase of $U_{\mathrm{m,m'}}(z)$ depending on the sign of the real number factor. Phase-flips are however rare, due to the persistence of the sign of the real number factor along the propagation coordinate.

The same phase behavior is observed for the 2D array of waveguides without NNN coupling ($C_d = 0$). In this case, we can write Eq. (6) in the following form:

$$U_{g(\mathrm{m,n}),g(\mathrm{m',n'})} = i^{\mathrm{m+n+m'+n'}} \sum_{\alpha,\gamma=0}^{\infty} (-1)^{\alpha\mu+\gamma\nu} \times H_{\mathrm{m,m',0,0},\alpha,\mu}(C_h, z) \cdot V_{\mathrm{n,n',0,0},\gamma,\nu}(C_v, z), \tag{11}$$

which can be recognized again as the product of a real number factor and the imaginary unit elevated to an integer exponent.

The very existence of the diagonal coupling (NNN interaction) has as a dramatic consequence for the phase of the input-response function. In fact, an inspection of Eq. (6) reveals that $C_d \neq 0$ entails that the summation over the indices k and l is not trivial. The field $U_{g(\mathrm{m,n}),g(\mathrm{m',n'})}$ results from the superposition of complex numbers, therefore the phase can in principle take any value in the interval $I = [0, 2\pi)$ along the propagation coordinate.

A numerical verification of the features of the input-response function discussed above is illustrated in Fig. 5, where the phase of the field in selected waveguides of a 5×5 array are plotted as a function of the propagation distance for different values of the ratio C_d/C_h. The excitation point of the array is in all cases site 1 (top-left waveguide, as seen from the output facet of the array). We see that in the case of no NNN interaction ($C_d = 0$), the phase of the input-response function is piecewise constant. The phase can flip by π only at few points along the propagation coordinate. A completely different scenario is observed as soon as we introduce a feeble diagonal coupling ($C_d = 0.025$). The phase is now varying smoothly while approximating the phase jumps observed in the case with no NNN interaction. For stronger diagonal coupling ($C_d = 0.25$), the phase dynamics of the input-response function is smooth and does not approximate any more the jumps of the $C_d = 0$ case.

V. PHASES OF THE INPUT-RESPONSE FUNCTION AND THE CONDITIONING OF THE α-MATRIX

With help of numerical simulations, I show now that the phase relationships within the input-response function are crucial to obtain low condition numbers for the α-matrix of the multi-field interferometer.

As an investigation tool, I use the statistical analysis of the condition number of randomly generated α-matrices. The matrices are generated by choosing randomly the square modulus and phase of the input-response function

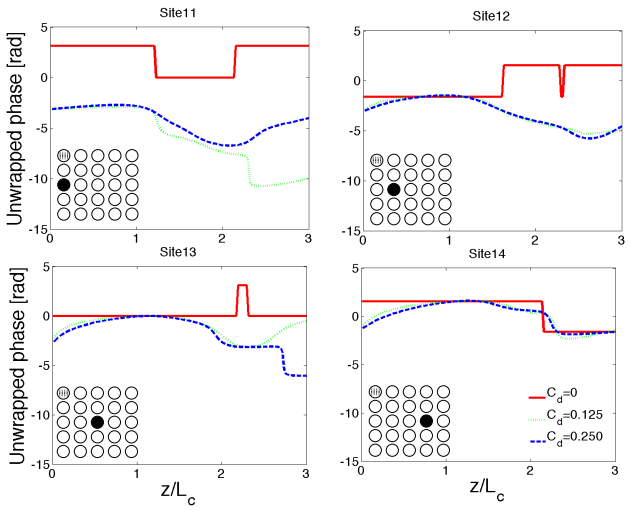

FIG. 5. (Color online) Phase of the output mode field for injection site 1 and observation sites 11-14. The insets represent the simulated configuration, as seen from the output facet of the array. Shaded waveguide: injection site. Black waveguide: observation site.

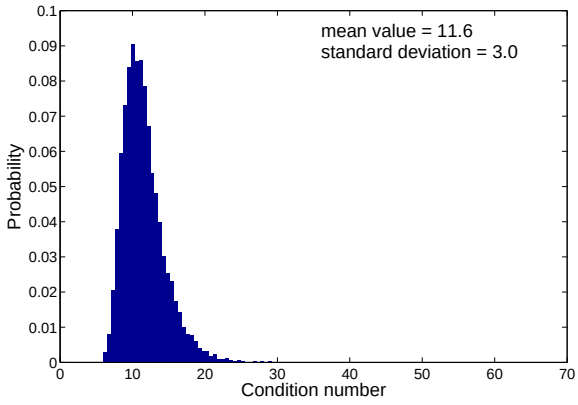

FIG. 6. Statistical distribution of the condition number of a random α-matrix featuring 25 instances of interferometric 4-field combination (equivalent to a 5×5 waveguides beam combiner). The histogram results from 10000 random matrix realizations.

$\{U\}$ of the waveguide array with $N = 25$ and $M = 4$. For each input field j, the distribution of the square modulus of the input-response function (A_{nj}) is chosen to be uniform in the interval $[0, 1]$ and then normalized to the total injected energy $E_j = \sum_{\mathrm{n}=1}^{N} A_{\mathrm{nj}}$. Similarly, for the input field j the N phases of $\{U_{\mathrm{nj}}\}$ are chosen to be uniformly distributed *i)* over the interval $[0, 2\pi)$ or, *ii)* over the discrete set of values $S = \{0, \pi/2, \pi, 3/2\pi\}$. If the distribution of the phases plays a role in the conditioning of the α-matrix, then we would expect that the average CN will be higher for the second case (phases chosen in a discrete interval).

Figure 6 illustrates the statistical distributions of the condition number of 10000 realizations of the random α-matrix for the case of phases of the input-response function distributed uniformly over the interval $[0, 2\pi)$. The distribution is peaked around a CN of 11, with an average value of CN=11.6 and a standard deviation of 3. The statistical distribution of the condition number for the case in which the phases of the input-response function are randomly chosen in the discrete set S is identical to the one of Fig. 6, and therefore not shown. This observation shows that the type of distribution of the phases of the input-response function does not impact the conditioning of the α-matrix, as long as the intensities of the same matrix are chosen randomly.

However, there is a further subtler issue related to the propagation of light in waveguide arrays without NNN coupling, namely that not only the phases of $\{U\}$ are chosen from a discrete set, but also that their pattern on the array is fixed by the geometry. This is evident from Eq. (10) and (11), where the complex pre-factor of the summation over the real functions is the imaginary unit elevated to an integer exponent equal to the sum of the site coordinates of the input waveguide and the observation waveguide. By implementing this symmetry in the generation of the random α-matrices, it turns out that the condition number becomes infinite for all the realizations. This symmetry of the phases is broken in the general case of light propagation in arrays with NNN coupling, due to the fact that the complex pre-factor is now multiplied by a complex number, rather than a real number (see Eq. (6)). The symmetry breaking is more pronounced as we increase the strength of the NNN coupling and the corresponding best α-matrix becomes more well conditioned.

VI. CONCLUSIONS

In conclusion, I have shown the impact of NNN-coupling on the conditioning of the matrix describing the multiple-field beam combination in an array of coupled waveguides. It was found empirically that arrays with no NNN-coupling cannot be used as DBC because the condition number of the α-matrix is infinite. On the contrary, NNN coupling allows the possibility to have finite condition numbers for all DBC configurations. Numerical search shows that a few among all the possible combinations of field injection and waveguide array length are well-conditioned (CN$<$ 10). Inspection of the intensities and phases of the elements of well- and ill-conditioned α-matrices shows that the conditioning is correlated to the distribution of phases. In particular, well-conditioned matrices have a greater phase diversity than ill-conditioned ones. I have shown how this fact is related to the analytical form of the input-response function of the waveguide array, whose phase characteristics change dramatically by adding NNN-coupling. Additionally, the numerical simulations based on randomly constructed α-matrices clearly point out that the NNN-coupling-induced symmetry breaking of the input-response function is necessary to use arrays of waveguides to retrieve simultaneously the correlation functions of several input fields. A corollary of these tests is that randomly constructed α-matrices perform in average significantly worse than the optimal configuration, suggesting that the optimal DBC configuration is not an approximation of a random interferometric beam combiner. While giving insight in the coherence properties of linearly coupled systems, these observations and findings have a direct impact on the design of multi-field interferometric beam combiners for applications ranging from astronomy to quantum optics and biosensors. Further impact of phase symmetry breaking operated by NNN could be foreseen for instance in the engineering of path-entangled quantum states of bi-photons propagating in 2D arrays of waveguides [21], or the understanding of the optical properties of multi-dimensional arrays of coupled plasmonic resonators (see *e.g.* [22]).

ACKNOWLEDGEMENTS

The author thanks Dr. Ottavia Jedrkiewicz for reading and commenting the manuscript. The work has been supported financially by the German Bundes-Ministerium für Bildung und Forschung, under contract 05A14SJA (project ALSI - Advanced Laser-writing for Stellar Interferometry).

[1] A. Glindemann, "Principles of Stellar Interferometry" (Springer, Berlin, 2013).
[2] U. Sinha, C. Couteau, T. Jennewein, R. Laflamme, and G. Weihs, Science **329**, 418 (2010).
[3] A. Ymeti, J. S. Kanger, J. Greve, P. V. Lambeck, R. Wijn, and R. G. Heideman, Appl. Opt. **42**, 5649 (2003).
[4] M. Benisty, J.-P. Berger, L. Jocoul, P. Labeye, F. Malbet, K. Perraut, and P. Kern, Astron. Astrophys. **498**, 601 (2009).
[5] S. Minardi and T. Pertsch Opt. Lett. **35**, 3009 (2010).
[6] S. Minardi, F. Dreisow, M. Gräfe, S. Nolte, and T. Pertsch, Opt. Lett. **37**, 3030 (2012).
[7] A. Saviauk, S. Minardi, F. Dreisow, S. Nolte, and T. Pertsch, Appl. Opt. **52**, 4556 (2013).
[8] S. Longhi, Laser & Photon. Rev. **3**, 243 (2009).
[9] M.C. Rechtsman, Julia M. Zeuner, A. Tünnermann, S. Nolte, M. Segev, and A. Szameit, Nat. Phot. **7**, 153 (2012).
[10] Y. Bromberg, Y. Lahini, R. Morandotti, and Y. Silberberg, Phys. Rev. Lett. **102**, 253904 (2009).
[11] D. Cheskis, S. Bar-Ad, R. Morandotti, J. S. Aitchison, H. S. Eisenberg, Y. Silberberg, and D. Ross, Phys. Rev. Lett. **91**, 223901 (2003).
[12] S. Minardi, F. Eilenberger, Y.V. Kartashov, A. Szameit, U. Röpke, J. Kobelke, K. Schuster, H. Bartelt, S. Nolte, L. Torner, F. Lederer, A. Tünnermann, and T. Pertsch, Phys. Rev. Lett. **105**, 263901 (2010).
[13] T. F. S. Büttner, D. D. Hudson, E. C. Mägi, A. C. Bedoya, T. Taunay, and B. J. Eggleton, Opt. Lett. **37**, 2469 (2012); S. Minardi, G. Cheng, C. D'Amico, and R. Stoian, Opt. Lett. **40**, 257 (2015).
[14] F. Dreisow, A. Szameit, M. Heinrich, T. Pertsch, S. Nolte, and A. Tünnermann, Opt. Lett. **33**, 2689 (2008).
[15] G. Corrielli, A. Crespi, G. Della Valle, S. Longhi, and R. Osellame, Nat. Comm. **4**, 1555 (2013).
[16] P. G. Kevrekidis, Phys. Lett. A **373**, 3688 (2009).
[17] D. N. Christodoulides, F. Lederer, and Y. Silberberg, Nature (London) **424**, 817 (2003).
[18] W. H. Press, S. A. Teukolsky, W. T. Vetterling, B. P. Flannery, "Numerical Recipes: the Art of Scientific Computing" (Cambridge University Press, Cambridge, 2007).
[19] S. Minardi, Mon. Not. R. Astron. Soc. **422**, 2656 (2012).
[20] A. Szameit, T. Pertsch, F. Dreisow, S. Nolte, A. Tünnermann, U. Peschel, and F. Lederer, Phys. Rev. A **75**, 053814 (2007).
[21] K. Poulios, R. Keil, D. Fry, J. D. A. Meinecke, J. C. F. Matthews, A. Politi, M. Lobino, M. Gräfe, M. Heinrich, S. Nolte, A. Szameit, and J. L. OBrien, Phys. Rev. Lett. **112**, 143604 (2014).
[22] D. P. Lyvers, J.-M. Moon, A. V. Kildishev, V. M. Shalaev, and A. Wei, ACS Nano **2**, 2569 (2008).